CHEMISTRY OF MATERIALS
Cite This: Chem. Mater. 2020, 32, 424−429
Article
pubs.acs.org/cm

Chemical Diversity in Lead-Free, Layered Double Perovskites: A Combined Experimental and Computational Approach

Brenda Vargas,[†,⊥] Raúl Torres-Cadena,[†,⊥] Diana T. Reyes-Castillo,[†] Joelis Rodríguez-Hernández,[‡] Milan Gembicky,[§] Eduardo Menéndez-Proupin,[∥] and Diego Solis-Ibarra*[,†]

[†]Laboratorio de Fisicoquímica y Reactividad de Superficies (LaFReS), Instituto de Investigaciones en Materiales, Universidad Nacional Autónoma de México, CU, Coyoacán, 04510 Ciudad de México, México

[‡]Centro de Investigación en Química Aplicada (CIQA), Blvd. Enrique Reyna Hermosillo, No. 140, Saltillo, Coahuila 25294, México

[§]Department of Chemistry and Biochemistry, University of California, San Diego, 9500 Gilman Drive, La Jolla, California 92093, United States

[∥]Grupo de Modelación de Materiales, Departamento de Física, Facultad de Ciencias, Universidad de Chile, Las Palmeras, 3425, Ñuñoa 780-0003, Santiago, Chile

Supporting Information

ABSTRACT: Akin to the expansion in compositional diversity that halide double perovskites provided to three-dimensional perovskites, layered double perovskites could further expand the diversity of two-dimensional (2D) perovskites, and therefore, they could also enhance the properties or expand the possible applications of such materials. Despite the great promise of halide 2D double perovskites, up to date, there are only four confirmed members of this family of materials. Herein, we explore 90 hypothetical new members of this family of materials by a combined theoretical, computational, and experimental method. The combination of these tactics allowed us to predict several new materials, out of which we experimentally synthesized and characterized five new layered double perovskites, some of which show promising properties for their use in photovoltaics and optoelectronics. Further, our work highlights the vast diversity of compositions and therefore of applications that double-layered perovskites have yet to offer.

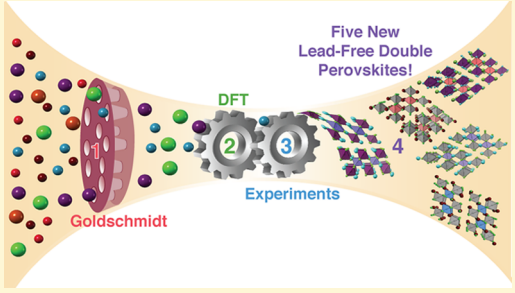

Lead halide perovskites have emerged as promising materials for optoelectronic applications.[1,2] Perhaps most prominently is their use in photovoltaic devices, which, in only 10 years, have reached power conversion efficiencies of up to 25.2%.[3] Despite significant efforts in this area, perovskite solar cells must overcome significant obstacles before their commercial use. Most notably are their lack of stability against light and moisture and the toxicity that these materials have due to the presence of lead.[4−9] Therefore, one of today's challenges is to find lead-free materials with similar properties, reduced toxicity, and improved stability.[10,11] Several different approaches and materials classes have been used to try to find lead-free alternatives to the three-dimensional (3D) $APbX_3$ perovskites, yet only moderate success has been achieved.[4−9] As single, "B-metal" perovskites yielded limited advances,[4−9] double perovskites with the formula $A_2M^IM^{III}X_6$ have garnered the attention of the scientific community, providing new possible metals and oxidation states and a very rich compositional diversity that in turn have resulted in promising new properties for their use in photovoltaic and optoelectronic applications.[10−26] Akin to what double perovskites have done for 3D halide perovskites, layered double perovskites have the potential to impact two-dimensional (2D) perovskites in a similar way: expanding the possible chemical space and possible properties of this already versatile family of materials.[27−31] Despite the great promise of this family of materials, to date, there are only four experimentally confirmed 2D double perovskites; thus, there is a need for further exploration of this family of perovskites.[29−35]

Recently, we have reported a new family of 2D halide double perovskites with the general formula $A_4M^{II}M^{III}{}_2X_{12}$, also known as the <111>-double perovskites.[29] Unlike, the traditional double perovskites, this family of perovskites incorporates divalent and trivalent metals in a two-dimensional (2D) structure. Further, they have shown to be remarkably stable toward humidity and light, to have appropriate band gaps for use in photovoltaics, and the ability to modulate their optical and magnetic properties.[29,32,36] Apart from these properties, there have been several computational efforts to predict other members of the <111>-double perovskite family.[37−40] Notably, several of these predicted materials have been proposed as absorbers for solar cells[37] or as p-type transparent conductors.[38] Despite all this interesting, proven, or predicted properties, to date, only two members of this family of

Received: September 30, 2019
Revised: December 10, 2019
Published: December 11, 2019

DOI: 10.1021/acs.chemmater.9b04021
Chem. Mater. 2020, 32, 424−429

materials have been experimentally demonstrated: $Cs_4CuSb_2Cl_{12}$ and $Cs_4MnSb_2Cl_{12}$. We, therefore, decided to explore 90 hypothetical new members of this family of materials by a combined theoretical, computational, and experimental method. The combination of these methodologies allowed us to predict several new hypothetical materials, out of which we were able to experimentally synthesize and characterize five new materials, some of which show promising properties for optoelectronic properties (Figure 1).

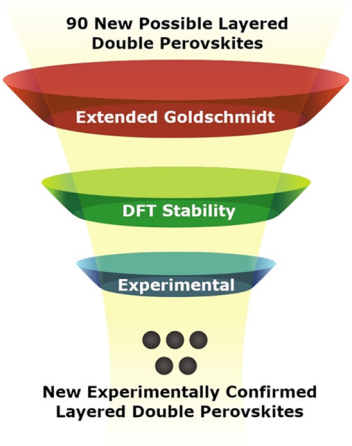

Figure 1. Schematic approach for the discovery of new <111>-oriented layered perovskites.

RESULTS AND DISCUSSION

Ionic Packing: Extended Goldschmidt. For the first part, we implemented Goldschmidt's empirical criterion. While this criterion was originally developed for AMX_3 perovskites, Xu et al. have recently extended this method for <111>-double perovskites.[38] Thus, it is possible to evaluate the viability of new hypothetical <111>-oriented perovskite structures with the form $A_4M^{II}M^{III}{}_2X_{12}$ in terms of ionic packing by using Goldschmidt's effective tolerance factor (t_{eff}) combined with the effective octahedral factor (μ_{eff}) according to eqs 1 and 2

$$t_{eff} = (R_A + R_X)/\sqrt{2}\,\{(R_{M^{II}} + 2R_{M^{III}})/3 + R_X\} \quad (1)$$

$$\mu_{eff} = (R_{M^{II}} + 2R_{M^{III}})/3R_X \quad (2)$$

where R_A, $R_{M^{II}}$, $R_{M^{III}}$, and R_X are the Shannon ionic radii. Thus, according to this approach, for a <111>-double perovskite to form, the effective tolerance factor requires to be between the values of $0.81 < t_{eff} < 1.11$ and the effective octahedral factor must be between the values of $0.41 < \mu_{eff} < 0.91$. Figure 2 shows the plotted values for the tolerance against the octahedral factor for perovskites with the formula $A_4M^{II}M^{III}{}_2X_{12}$ (A = Rb^+ and Cs^+; M^{II} = Ti^{2+}, V^{2+}, Cr^{2+}, Mn^{2+}, Fe^{2+}, Co^{2+}, Ni^{2+}, Cu^{2+}, Zn^{2+}, and Cd^{2+}; M^{III} = Sb^{3+} and Bi^{3+}; X^- = Cl^-, Br^-, and I^-). From these graphs, for the antimony-based materials (Figure 2A,B), it can be observed that most chlorides lie between the desired values, whereas $Cs_4CdSb_2Br_{12}$ is the only antimony–bromide material that satisfies these criteria and no iodide-containing material fulfills both parameters when M^{III} is antimony. This can be rationalized when considering the longer metal–halide bond distance that heavier halides have, which translate into the need for bigger cations to stabilize a <111>-double perovskite structure. On the other hand, for Bi^{3+} perovskites (Figure 2C), all of the 30 combinations tested lie within the stable perovskite zone. The latter can be attributed to the larger Bi–X bonds but also raises the question of whether the stability limits established for these perovskites should be re-evaluated. The latter further heightens the need for more experimentally confirmed members of this family of materials, which could help to better predict possible members of this family of materials.

Relative Thermodynamic Stability. Once we were able to discriminate among the 90 possible materials using ionic packing criteria, we then evaluated the stability of formation of the 25 remaining chloride–antimony- and bismuth–chloride-based candidates. For the time being and due to computational restrictions, we limited our explorations to chloride-based perovskites. Therefore, we calculated the formation energies of the new possible perovskites and compared them with the energies of all known binary and ternary possible decomposition products (Figure 3). In all the cases where transition metals are present, and in order to better predict formation energies, we considered the magnetic configurations of such materials (see the Supporting Information for details). The only materials considered as diamagnetic compounds are Zn and Cd perovskites. As additional validation, we included the already synthesized copper and manganese perovskite compounds. For all perovskites, the decomposition pathway used were the binary compounds (Figure 3, green bars), the

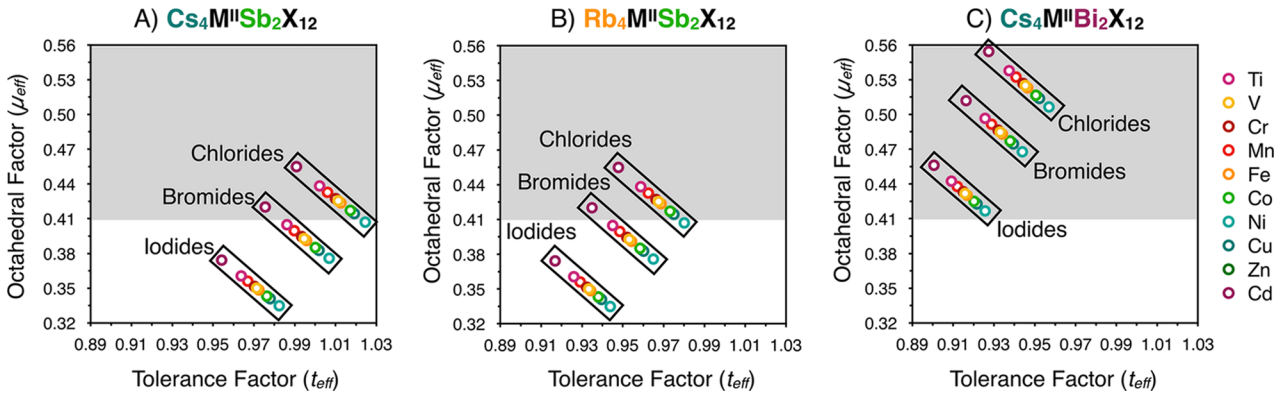

Figure 2. t_{eff} vs μ_{eff} of 90 $A_4M^{II}M^{III}{}_2X_{12}$. The gray area indicates stable areas of the perovskite structures: (A) $Cs_4M^{II}Sb_2X_{12}$; (B) $Rb_4M^{II}Sb_2X_{12}$; (C) $Cs_4M^{II}Bi_2X_{12}$.

DOI: 10.1021/acs.chemmater.9b04021
Chem. Mater. 2020, 32, 424–429

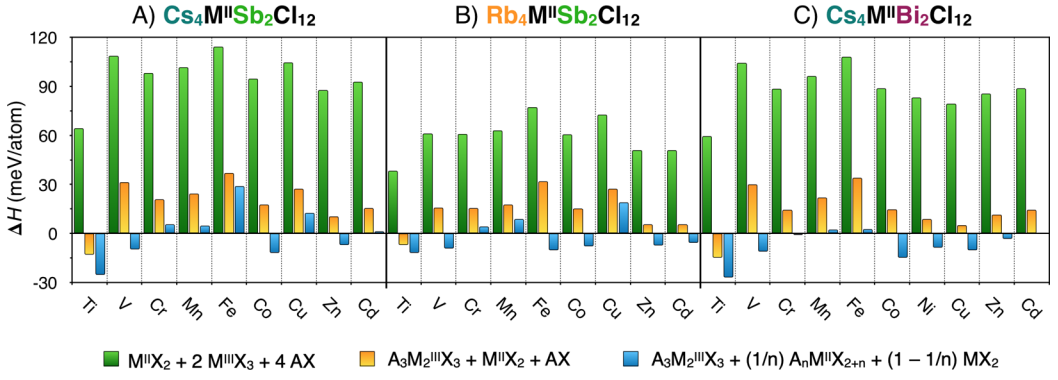

Figure 3. DFT-calculated relative energies of decomposition reactions for 28 $A_4M^{II}M^{III}{}_2X_{12}$. In the case of M^{II} = Ti, V, Mn, Fe, Co, Ni, Cu, and Cd, $AM^{II}X_3$ was used as the ternary compound; otherwise, when M^{II} = Cr and Zn, $A_2M^{II}X_4$ was used as the ternary compound: (A) $Cs_4M^{II}Sb_2Cl_{12}$; (B) $Rb_4M^{II}Sb_2Cl_{12}$; (C) $Cs_4M^{II}Bi_2Cl_{12}$.

double perovskite $A_3M^{III}{}_2X_9$ and a mixture of ternary and binary compounds (Figure 3, yellow bars), and finally a ternary perovskite phase and two binary compounds (Figure 3, blue bars).

From these results, it first shall be noted that both $Cs_4CuSb_2Cl_{12}$ and $Cs_4MnSb_2Cl_{12}$, which are the only two experimentally confirmed members of this family of materials, are calculated to be stable according to our approach, which is the first validation that our approach is apt for predicting stability of this family of materials. Second, our method predicted that, out of the 28 candidates, 17 of these are not thermodynamically favorable and only 9 are likely to form. This gave a reasonable set of experimental targets, and more precisely, we decided to experimentally attempt to synthesize $Cs_4FeSb_2Cl_{12}$, $Cs_4CrSb_2Cl_{12}$, $Rb_4CrSb_2Cl_{12}$, $Rb_4MnSb_2Cl_{12}$, $Rb_4CuSb_2Cl_{12}$, $Cs_4CdSb_2Cl_{12}$, $Cs_4MnBi_2Cl_{12}$, $Cs_4FeBi_2Cl_{12}$, and $Cs_4CdBi_2Cl_{12}$. Our results in the latter endeavor are described in the following section. It is noteworthy that, according to the band diagram of these nine new materials, all of them except for $Rb_4CuSb_2Cl_{12}$ are predicted to be wide-band-gap semiconductors, with band gaps ranging from 2.7 to 3.6 eV (Figures S1 and S2 and Table S5). On the other hand, $Rb_4CuSb_2Cl_{12}$ is predicted to have a band gap of 1.7 eV and a density of states reminiscent to that of $Cs_4CuSb_2Cl_{12}$,[32] with a bottom of the conduction band mostly composed of copper d orbitals. Importantly, two of the predicted materials, $Cs_4CdSb_2Cl_{12}$ and $Cs_4CdBi_2Cl_{12}$, were also predicted to be stable, direct band gap semiconductors by Huang and co-workers.[38]

Experimental Discovery of New <111>-Oriented Layered Perovskites. The attempts to synthesize the targeted compounds were done by either a solid-state reaction or by precipitation in methanolic or acid solutions (see the Material Synthesis section of the Supporting Information). Ultimately, we were able to synthesize five new $A_4MB_2Cl_{12}$ materials, namely, $Cs_4CdSb_2Cl_{12}$, $Rb_4MnSb_2Cl_{12}$, $Rb_4CuSb_2Cl_{12}$, $Cs_4MnBi_2Cl_{12}$, and $Cs_4CdBi_2Cl_{12}$. On the other hand, we were not able to synthesize chromium-containing materials ($Cs_4CrSb_2Cl_{12}$ and $Rb_4CrSb_2Cl_{12}$) or iron-containing materials ($Cs_4FeSb_2Cl_{12}$ and $Cs_4FeBi_2Cl_{12}$). The lack of success synthesizing these materials could be partially ascribed to the difficulty of maintaining such metals in a 2+ oxidation state, big differences in solubilities, or alternatively inadequate synthetic conditions.

Similar to the previously reported materials, the new copper-containing perovskite ($Rb_4CuSb_2Cl_{12}$) and the two manganese-containing materials ($Rb_4MnSb_2Cl_{12}$ and $Cs_4MnBi_2Cl_{12}$) are black (Cu) or pale pink crystalline solids (Mn), respectively. The cadmium-containing structures ($Cs_4CdSb_2Cl_{12}$ and $Cs_4CdBi_2Cl_{12}$) are colorless microcrystalline solids. The structures of the Cs-containing materials ($Cs_4CdSb_2Cl_{12}$, $Cs_4MnBi_2Cl_{12}$, and $Cs_4CdBi_2Cl_{12}$) were determined by powder X-ray diffraction (Tables S3–S5). Importantly, all of the structures have the predicted <111>-oriented layered perovskite structure (Figure 4) and share the

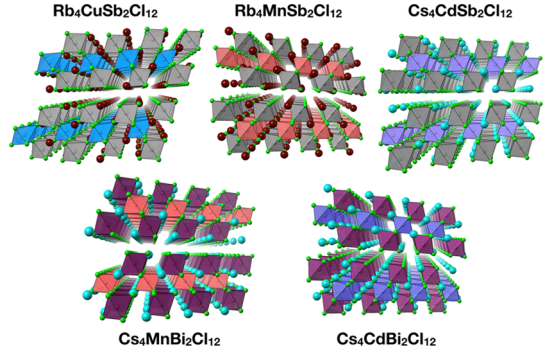

Figure 4. Structures of $Rb_4CuSb_2Cl_{12}$, $Rb_4MnSb_2Cl_{12}$, $Cs_4CdSb_2Cl_{12}$, $Cs_4MnBi_2Cl_{12}$, and $Cs_4CdBi_2Cl_{12}$ from left to right and top to bottom respectively. Cl, Rb, and Cs atoms are depicted as green, brown, and purple spheres, respectively; Sb, Cu, Mn, Bi, and Cd coordination polyhedra are shown in gray, blue, pink, wine, and lavender, respectively.

$R\bar{3}m$ space group. On the other hand, we were not able to determine the structures of the Rb-containing materials ($Rb_4MnSb_2Cl_{12}$ and $Rb_4CuBi_2Cl_{12}$) since they show to be unstable toward X-ray radiation. Despite the latter, quick scans allowed us to determine the unit cell and possible space groups (see Table S6), both of which are consistent with the formation of the desired double perovskites. As expected, bigger elements (Cd and Bi) yield larger unit cells, and smaller ones (Cu, Mn, and Sb) result in smaller unit cells (see Table S3).

The cesium-containing perovskites, namely, $Cs_4CdSb_2Cl_{12}$, $Cs_4MnBi_2Cl_{12}$, and $Cs_4CdBi_2Cl_{12}$, have excellent stability toward heat, with decomposition temperatures above 200 °C and up to 350 °C, with no observable phase transitions from −85 to 200 or 300 °C, respectively (Figures S5 and S6). Further, they also tolerate humidity and light irradiation quite well, and even after exposure to ambient conditions for up to 7

DOI: 10.1021/acs.chemmater.9b04021
Chem. Mater. 2020, 32, 424−429

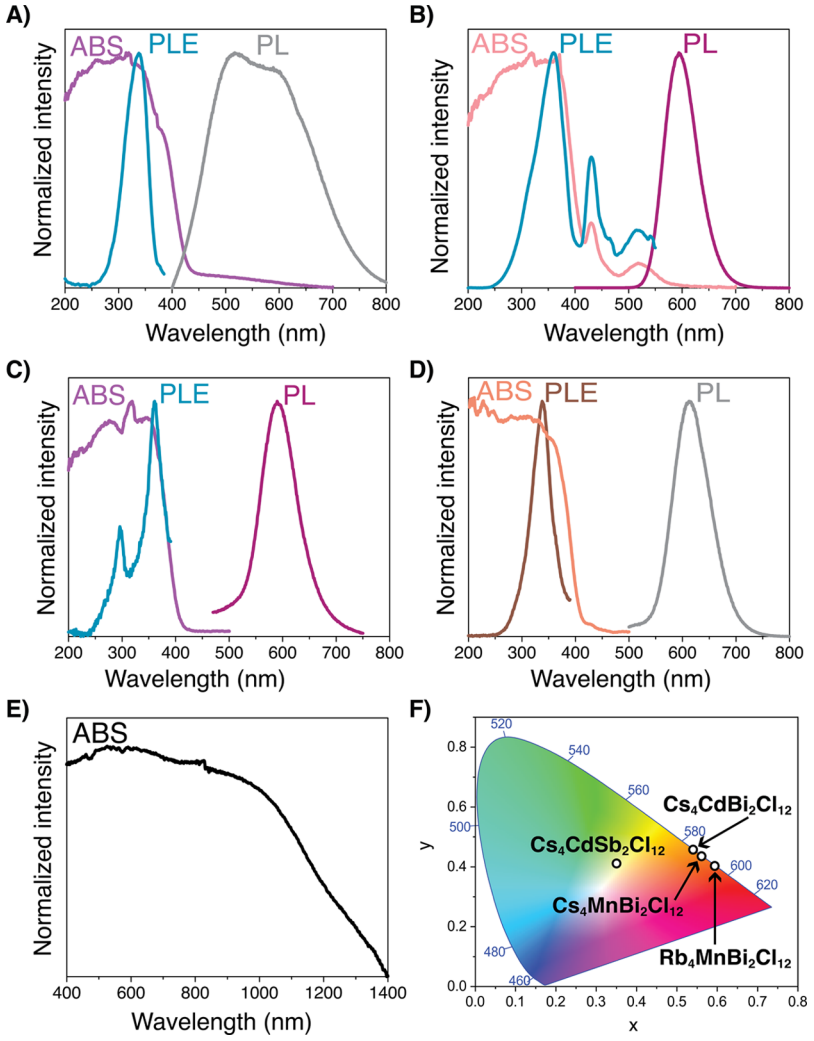

Figure 5. Absorption, photoluminescence, and excitation spectra of (A) $Cs_4CdSb_2Cl_{12}$, (B) $Cs_4MnBi_2Cl_{12}$, (C) $Cs_4CdBi_2Cl_{12}$, and (D) $Rb_4MnBi_2Cl_{12}$. (E) Absorbance spectrum of $Cs_4CdSb_2Cl_{12}$. Panel (F) shows the chromaticity diagram of $Cs_4CdSb_2Cl_{12}$, $Cs_4MnBi_2Cl_{12}$, $Cs_4CdBi_2Cl_{12}$, and $Rb_4MnBi_2Cl_{12}$.

months, we see no sign of decomposition (Figure S8). Conversely, the Rb-containing materials, $Rb_4MnSb_2Cl_{12}$ and $Rb_4CuSb_2Cl_{12}$, resulted in less stable solids, both toward heat and humidity (Figures S7 and S9), presumably due to the more hygroscopic and more volatile nature of rubidium salts.

In terms of optical properties, all but $Rb_4CuSb_2Cl_{12}$ present absorption characteristics of a wide-band-gap semiconductor, with band gaps close to 3.0 eV (Figure 5 and Table S7). On the other hand, $Rb_4CuSb_2Cl_{12}$ is a black solid microcrystalline solid with a much smaller direct band gap of about 0.9 eV. Such a small band gap is on a par with the previously reported $Cs_4CuSb_2Cl_{12}$, which has a band gap of 1.0 eV[29] and is consistent with previous calculations[38] that suggest that the A cation does not play a significant role near the band edges of these materials. While the previous literature would suggest that most, if not all, of these materials have direct band gaps, further studies are needed in order to unequivocally determine the nature of the band gap: direct or indirect.

Finally, we studied the steady-state photoluminescence (PL) of the newly discovered materials (Figure 5). All of the materials, except for $Rb_4CuSb_2Cl_{12}$, exhibited relative broad PL emissions; particularly, $Cs_4CdSb_2Cl_{12}$ exhibited a very broad PL signal that spans all the visible spectra with a full width at half-maximum (FWHM) of 220 nm. Due to the broadness of its emission, $Cs_4CdSb_2Cl_{12}$ can be classified as a white-light emitter with CIE coordinates that are typically considered "warm" white light (Figure 5F). The broad PL signals could be attributed to the presence of self-trapped excitons (STEs), similar to what has been recently observed in several metal–halides.[41−49]

Given the observed PL and 2D nature of these materials, they are promising candidates for optoelectronic applications. Other interesting possibility is to test some of these materials as conducting transparent materials. In fact, Huang and co-workers predicted $Cs_4CdSb_2Cl_{12}$ and related materials to have excellent properties for their use as p-type transparent conductors.[38]

■ CONCLUSIONS

Despite their promising properties, before this work, the layered double perovskite family consisted of only four confirmed members. Herein, using a mixed computational and experimental approach, we have predicted and corroborated five new double <111>-oriented layered perovskites, some of which show promising properties for optoelectronic applications. Perhaps more importantly, we have shown how

DOI: 10.1021/acs.chemmater.9b04021
Chem. Mater. 2020, 32, 424−429

this family of double layered perovskites has an enormous chemical versatility, which should in turn result in tremendous potential for the discovery of new lead-free materials for photovoltaic and optoelectronic applications. Here, in particular, we have shown that it is possible to replace the A, M^{II}, and M^{III} sites out of the canonical formula $A_4M^{II}M^{III}{}_2X_{12}$. Further studies to explore the properties and possible applications of these materials, as well as to extend the possible metals and halides capable of forming these kinds of materials, are underway in our laboratories.

■ ASSOCIATED CONTENT

Supporting Information

The Supporting Information is available free of charge at https://pubs.acs.org/doi/10.1021/acs.chemmater.9b04021.

Complete experimental and computational details, Figures S1−S11 and Tables S1−S10 (PDF)

■ AUTHOR INFORMATION

Corresponding Author

*E-mail: diego.solis@unam.mx.

ORCID

Diego Solis-Ibarra: 0000-0002-2486-0967

Author Contributions

⊥B.V. and R.T.-C. contributed equally.

Funding

We acknowledge the financial support from PAPIIT IA202418 and CONACYT's CB-A1-S-8729. E.M.-P. acknowledges support by CONICYT/FONDECYT Regular Grant 1171807. Powered@NLHPC: This research was partially supported by the supercomputing infrastructure of the NLHPC (ECM-02).

Notes

The authors declare no competing financial interest.

■ ACKNOWLEDGMENTS

We acknowledge the financial support from PAPIIT IA202418 and CONACYT's CB-A1-S-8729. E.M.-P. acknowledges support by CONICYT/FONDECYT Regular Grant 1171807. Powered@NLHPC: This research was partially supported by the supercomputing infrastructure of the NLHPC (ECM-02). We also thank Adriana Tejeda, Carlos Ramos, Eriseth Morales, Alberto López, Alejandro Pompa, Cain González, and Miguel Angel Canseco for technical assistance.

■ REFERENCES

(1) Stranks, S. D.; Snaith, H. J. Metal-halide Perovskites for Photovoltaic and Light-Emitting Devices. *Nat. Nanotechnol.* **2015**, *10*, 391−402.

(2) Zhang, W.; Eperon, G. E.; Snaith, H. J. Metal Halide Perovskites for Energy Applications. *Nat. Energy* **2016**, *1*, 16048.

(3) National Renewable Laboratory *Best Research-Cell Efficiency Chart*; https://www.nrel.gov/pv/cell-efficiency.html, (accessed December 7, 2019).

(4) Hao, F.; Stoumpos, C. C.; Cao, D. H.; Chang, R. P. H.; Kanatzidis, M. G. Lead-Free Solid-State Organic-Inorganic Halide Perovskite Solar Cells. *Nat. Photonics* **2014**, *8*, 489−494.

(5) Ju, M.-G.; Dai, J.; Ma, L.; Zeng, X. C. Lead-Free Mixed Tin and Germanium Perovskites for Photovoltaic Application. *J. Am. Chem. Soc.* **2017**, *139*, 8038−8043.

(6) Ke, W.; Kanatzidis, M. G. Prospects For Low-Toxicity Lead-Free Perovskite Solar Cells. *Nat. Commun.* **2019**, *10*, 965.

(7) Ke, W.; Stoumpos, C. C.; Spanopoulos, I.; Mao, L.; Chen, M.; Wasielewski, M. R.; Kanatzidis, M. G. Efficient Lead-Free Solar Cells Based on Hollow {en}$MASnI_3$ Perovskites. *J. Am. Chem. Soc.* **2017**, *139*, 14800−14806.

(8) Kim, H.; Lee, Y. H.; Lyu, T.; Yoo, J. H.; Park, T.; Oh, J. H. Boosting The Performance And Stability Of Quasi-Two-Dimensional Tin-Based Perovskite Solar Cells Using The Formamidinium Thiocyanate Additive. *J. Mater. Chem. A* **2018**, *6*, 18173−18182.

(9) Noel, N. K.; Stranks, S. D.; Abate, A.; Wehrenfennig, C.; Guarnera, S.; Haghighirad, A.-A.; Sadhanala, A.; Eperon, G. E.; Pathak, S. K.; Johnston, M. B.; et al. Lead-Free Organic-Inorganic Tin Halide Perovskites For Photovoltaic Applications. *Energy Environ. Sci.* **2014**, *7*, 3061−3068.

(10) Chakraborty, S.; Xie, W.; Mathews, N.; Sherburne, M.; Ahuja, R.; Asta, M.; Mhaisalkar, S. G. Rational Design: A High-Throughput Computational Screening and Experimental Validation Methodology for Lead-Free and Emergent Hybrid Perovskites. *ACS Energy Lett.* **2017**, *2*, 837−845.

(11) Giustino, F.; Snaith, H. J. Toward Lead-Free Perovskite Solar Cells. *ACS Energy Lett.* **2016**, *1*, 1233−1240.

(12) Askerka, M.; Li, Z.; Lempen, M.; Liu, Y.; Johnston, A.; Saidaminov, M. I.; Zajacz, Z.; Sargent, E. H. Learning-in-Templates Enables Accelerated Discovery and Synthesis of New Stable Double Perovskites. *J. Am. Chem. Soc.* **2019**, *141*, 3682−3690.

(13) Bekenstein, Y.; Dahl, J. C.; Huang, J.; Osowiecki, W. T.; Swabeck, J. K.; Chan, E. M.; Yang, P.; Alivisatos, A. P. The Making and Breaking of Lead-Free Double Perovskite Nanocrystals of Cesium Silver-Bismuth Halide Compositions. *Nano Lett.* **2018**, *18*, 3502−3508.

(14) Savory, C. N.; Walsh, A.; Scanlon, D. O. Can Pb-Free Halide Double Perovskites Support High-Efficiency Solar Cells? *ACS Energy Lett.* **2016**, *1*, 949−955.

(15) Slavney, A. H.; Hu, T.; Lindenberg, A. M.; Karunadasa, H. I. A Bismuth-Halide Double Perovskite with Long Carrier Recombination Lifetime for Photovoltaic Applications. *J. Am. Chem. Soc.* **2016**, *138*, 2138−2141.

(16) Slavney, A. H.; Leppert, L.; Bartesaghi, D.; Gold-Parker, A.; Toney, M. F.; Savenije, T. J.; Neaton, J. B.; Karunadasa, H. I. Defect-Induced Band-Edge Reconstruction of a Bismuth-Halide Double Perovskite for Visible-Light Absorption. *J. Am. Chem. Soc.* **2017**, *139*, 5015−5018.

(17) Tran, T. T.; Panella, J. R.; Chamorro, J. R.; Morey, J. R.; McQueen, T. M. Designing Indirect-Direct Bandgap Transitions In Double Perovskites. *Mater. Horiz.* **2017**, *4*, 688−693.

(18) Volonakis, G.; Filip, M. R.; Haghighirad, A. A.; Sakai, N.; Wenger, B.; Snaith, H. J.; Giustino, F. Lead-Free Halide Double Perovskites via Heterovalent Substitution of Noble Metals. *J. Phys. Chem. Lett.* **2016**, *7*, 1254−1259.

(19) Volonakis, G.; Haghighirad, A. A.; Milot, R. L.; Sio, W. H.; Filip, M. R.; Wenger, B.; Johnston, M. B.; Herz, L. M.; Snaith, H. J.; Giustino, F. $Cs_2InAgCl_6$: A New Lead-Free Halide Double Perovskite with Direct Band Gap. *J. Phys. Chem. Lett.* **2017**, *8*, 772−778.

(20) Wei, F.; Deng, Z.; Sun, S.; Xie, F.; Kieslich, G.; Evans, D. M.; Carpenter, M. A.; Bristowe, P. D.; Cheetham, A. K. The Synthesis, Structure And Electronic Properties Of A Lead-Free Hybrid Inorganic-Organic Double Perovskites (MA)2KBiCl6 (MA=methy-lammonium). *Mater. Horiz.* **2016**, *3*, 328−332.

(21) Creutz, S. E.; Crites, E. N.; De Siena, M. C.; Gamelin, D. R. Colloidal Nanocrystals of Lead-Free Double-Perovskite (Elpasolite) Semiconductors: Synthesis and Anion Exchange To Access New Materials. *Nano Lett.* **2018**, *18*, 1118−1123.

(22) Locardi, F.; Cirignano, M.; Baranov, D.; Dang, Z.; Prato, M.; Drago, F.; Ferretti, M.; Pinchetti, V.; Fanciulli, M.; Brovelli, S.; et al. Colloidal Synthesis of Double Perovskite $Cs_2AgInCl_6$ and Mn-Doped $Cs_2AgInCl_6$ Nanocrystals. *J. Am. Chem. Soc.* **2018**, *140*, 12989−12995.

(23) Luo, J.; Wang, X.; Li, S.; Liu, J.; Guo, Y.; Niu, G.; Yao, L.; Fu, Y.; Gao, L.; Dong, Q.; et al. Efficient And Stable Emission Of Warm-

White Light From Lead-Free Halide Double Perovskites. *Nature* **2018**, *563*, 541−545.
(24) Majher, J. D.; Gray, M. B.; Strom, T. A.; Woodward, P. M. $Cs_2NaBiCl_6$:Mn^{2+}-A New Orange-Red Halide Double Perovskite Phosphor. *Chem. Mater.* **2019**, *31*, 1738−1744.
(25) Deng, W.; Deng, Z.-Y.; He, J.; Wang, M.; Chen, Z.-X.; Wei, S.-H.; Feng, H.-J. Synthesis of $Cs_2AgSbCl_6$ and improved Optoelectronic Properties Of $Cs_2AgSbCl_6/TiO_2$ Heterostructure Driven By The Interface Effect For Lead-Free Double Perovskites Solar Cells. *Appl. Phys. Lett.* **2017**, *111*, 151602.
(26) Deng, Z.; Wei, F.; Sun, S.; Kieslich, G.; Cheetham, A. K.; Bristowe, P. D. Exploring The Properties Of Lead-Free Hybrid Double Perovskites Using A Combined Computational-Experimental Approach. *J. Mater. Chem. A* **2016**, *4*, 12025−12029.
(27) Karmakar, A.; Dodd, M. S.; Agnihotri, S.; Ravera, E.; Michaelis, V. K. Cu(II)-Doped $Cs_2SbAgCl_6$ Double Perovskite: A Lead-Free, Low-Bandgap Material. *Chem. Mater.* **2018**, *30*, 8280−8290.
(28) Meng, W.; Wang, X.; Xiao, Z.; Wang, J.; Mitzi, D. B.; Yan, Y. Parity-Forbidden Transitions and Their Impact on the Optical Absorption Properties of Lead-Free Metal Halide Perovskites and Double Perovskites. *J. Phys. Chem. Lett.* **2017**, *8*, 2999−3007.
(29) Vargas, B.; Ramos, E.; Pérez-Gutiérrez, E.; Alonso, J. C.; Solis-Ibarra, D. A Direct Bandgap Copper-Antimony Halide Perovskite. *J. Am. Chem. Soc.* **2017**, *139*, 9116−9119.
(30) Connor, B. A.; Leppert, L.; Smith, M. D.; Neaton, J. B.; Karunadasa, H. I. Layered Halide Double Perovskites: Dimensional Reduction of $Cs_2AgBiBr_6$. *J. Am. Chem. Soc.* **2018**, *140*, 5235−5240.
(31) Ortiz-Cervantes, C.; Carmona-Monroy, P.; Solis-Ibarra, D. Two-Dimensional Halide Perovskites in Solar Cells: 2D or not 2D? *ChemSusChem* **2019**, *12*, 1560−1575.
(32) Vargas, B.; Torres-Cadena, R.; Rodríguez-Hernández, J.; Gembicky, M.; Xie, H.; Jiménez-Mier, J.; Liu, Y.-S.; Menéndez-Proupin, E.; Dunbar, K. R.; Lopez, N.; et al. Optical, Electronic, and Magnetic Engineering of <111> Layered Halide Perovskites. *Chem. Mater.* **2018**, *30*, 5315−5321.
(33) During revisions of the present manuscript, we became aware of two new relevant publications (refs 34 and 35), which increased the number of reported layered double perovskites. Most notably, ref 34 reports the synthesis of two of the materials included herein: $Cs_4CdSb_2Cl_{12}$ and $Cs_4CdBi_2Cl_{12}$. Nevertheless, these materials were obtained by a different method and with some differences in the computational and experimental results.
(34) Lin, Y.-P.; Hu, S.; Xia, B.; Fan, K.-Q.; Gong, L.-K.; Kong, J.-T.; Huang, X.-Y.; Xiao, Z.; Du, K.-Z. Material Design and Optoelectronic Properties of Three-Dimensional Quadruple Perovskite Halides. *J. Phys. Chem. Lett.* **2019**, *10*, 5219−5225.
(35) Mao, L.; Teicher, S. M. L.; Stoumpos, C. C.; Kennard, R. M.; DeCrescent, R. A.; Wu, G.; Schuller, J. A.; Chabinyc, M. L.; Cheetham, A. K.; Seshadri, R. Chemical and Structural Diversity of Hybrid Layered Double Perovskite Halides. *J. Am. Chem. Soc.* **2019**, 19099.
(36) Singhal, N.; Chakraborty, R.; Ghosh, P.; Nag, A. Low-Bandgap $Cs_4CuSb_2Cl_{12}$ Layered Double Perovskite: Synthesis, Reversible Thermal Changes, and Magnetic Interaction. *Chem. - Asian J.* **2018**, *13*, 2085−2092.
(37) Tang, G.; Xiao, Z.; Hosono, H.; Kamiya, T.; Fang, D.; Hong, J. Layered Halide Double Perovskites $Cs_{3+n}M(II)_nSb_2X_{9+3n}$ (M=Sn, Ge) for Photovoltaic Applications. *J. Phys. Chem. Lett.* **2018**, *9*, 43−48.
(38) Xu, J.; Liu, J.-B.; Wang, J.; Liu, B.-X.; Huang, B. Prediction of Novel*p*-Type Transparent Conductors in Layered Double Perovskites: A First-Principles Study. *Adv. Funct. Mater.* **2018**, *28*, 1800332.
(39) Liu, Z.; Zhao, X.; Zunger, A.; Zhang, L. Design of Mixed-Cation Tri-Layered Pb-Free Halide Perovskites for Optoelectronic Applications. *Adv. Electron. Mater.* **2019**, *5*, 1900234.
(40) Xu, J.; Xu, C.; Liu, J.-B.; et al. Prediction of room-temperature half-metallicity in layered halide double perovskites. *npj Comput. Mater.* **2019**, 114.
(41) Cortecchia, D.; Yin, J.; Petrozza, A.; Soci, C. White Light Emission In Low-Dimensional Perovskites. *J. Mater. Chem. C* **2019**, *7*, 4956−4969.
(42) Dohner, E. R.; Hoke, E. T.; Karunadasa, H. I. Self-Assembly of Broadband White-Light Emitters. *J. Am. Chem. Soc.* **2014**, *136*, 1718−1721.
(43) Dohner, E. R.; Jaffe, A.; Bradshaw, L. R.; Karunadasa, H. I. Intrinsic White-light Emission from Layered Hybrid Perovskites. *J. Am. Chem. Soc.* **2014**, *136*, 13154−13157.
(44) Hamada, Y.; Sano, T.; Fujii, H.; Nishio, Y.; Takahashi, H.; Shibata, K. White-Light-Emitting Material for Organic Electroluminiscent Devices. *Jpn. J. Appl. Phys.* **1996**, *35*, L1339−L1341.
(45) Hu, T.; Smith, M. D.; Dohner, E. R.; Sher, M.-J.; Wu, X.; Trinh, M. T.; Fisher, A.; Corbett, J.; Zhu, X.-Y.; Karunadasa, H. I.; et al. Mechanism for Broadband White-Light Emission from Two-Dimensional (110) Hybrid Perovskites. *J. Phys. Chem. Lett.* **2016**, *7*, 2258−2263.
(46) Mao, L.; Wu, Y.; Stoumpos, C. C.; Wasielewski, M. R.; Kanatzidis, M. G. White-Light Emission and Structural Distortion in New Corrugated Two-Dimensional Lead Bromide Perovskites. *J. Am. Chem. Soc.* **2017**, *139*, 5210−5215.
(47) Smith, M. D.; Karunadasa, H. I. White-Light Emission from Layered Halide Perovskites. *Acc. Chem. Res.* **2018**, *51*, 619−627.
(48) Yuan, Z.; Zhou, C.; Tian, Y.; Shu, Y.; Messier, J.; Wang, J. C.; van de Burgt, L. J.; Kountouriotis, K.; Xin, Y.; Holt, E.; et al. One-dimensional organic lead halide perovskites with efficient bluish white-light emission. *Nat. Commun* **2017**, *8*, 14051.
(49) Yangui, A.; Roccanova, R.; McWhorter, T. M.; Wu, Y.; Du, M.-H.; Saparov, B. Hybrid Organic-Inorganic Halides $(C_5H_7N_2)_2MBr_4$ (M=Hg, Zn) with High Color Rendering Index and High-Efficiency White-Light Emission. *Chem. Mater.* **2019**, *31*, 2983−2991.

DOI: 10.1021/acs.chemmater.9b04021
Chem. Mater. 2020, 32, 424−429